Sequestration of cadmium and zinc in Ca-containing grains excreted by tobacco

Marie-Pierre Isaure[1], Géraldine Sarret[1], Emiko Harada[1, 2, 3], Yong-Eui Choi [2], Matthew A. Marcus [4], Jean Susini [5], Stephan Clemens [3], and Alain Manceau[1]

[1] Environmental Geochemistry Group, LGIT, University of Grenoble and CNRS, BP 53, 38041 Grenoble Cedex 9, France
[2] Division of Forestry Resources, College of Forest Sciences, Kangwon National University, Chunchon 200-701, Kangwon-do, Korea
[3] Leibniz-Institut für Pflanzenbiochemie, Weinberg 3, 06120 Halle (Saale), Germany
[4] Advanced Light Source (ALS), Berkeley Lab, MS 6-2100, Berkeley, CA 94720, USA
[5] ESRF, ID21, BP 220, 38043 Grenoble, France

ABSTRACT

In tobacco exposed to Zn and Cd, trichomes were found to excrete micrometer-sized Ca/Zn and Ca/Cd-containing grains. In this study, we clarified the mechanism of Cd and Zn sequestration in these grains using a combination of laterally resolved techniques : scanning electron microscopy coupled with X-ray analysis (SEM-EDX), microfocused X-ray diffraction (µXRD), and microfocused X-ray absorption spectroscopies (µXANES and µEXAFS). For Zn + Ca exposition, substituted calcite was the most frequent excreted mineral, and Zn species identified by µEXAFS were Zn-substituted calcite as major form and Zn bound to organic compounds, Zn-containing silica and phosphate as minor species. Under Cd + Ca exposition, plants excreted mostly spherular particles composed of Cd-enriched substituted vaterite and to a lesser extent faceted grains less concentrated with Cd and composed of substituted calcite. Cd L_{III}-edge µXANES evidenced Cd-substituted vaterite in spherular grains and Cd-substituted calcite in faceted grains. This novel mechanism of Cd and Zn detoxification has health and environmental significances for smokers and phytoremediation. This study also illustrates the complementarity of µXRD and µEXAFS/µXANES techniques to examine metal speciation in biogenic products.

INTRODUCTION

Plants develop various mechanisms to tolerate heavy metals in their tissues. Recently, tobacco (*Nicotiana tabacum*) was shown to detoxify Cd^{2+} by excreting Ca/Cd-containing grains through their trichomes (epidermal hairs) (Choi et al., 2001; Choi et al., 2004). In this study, we have shown that Ca has a protective effect against Zn toxicity (Fig. 1) and that exposure to Zn induced an increase in the trichome density and an excretion of Ca/Zn-containing grains (Figs. 2 and 3). In order to better understand the mechanism of metal sequestration and excretion, the morphology and chemical composition of the Ca/Cd- and Ca/Zn- grains were studied by scanning electron microscopy coupled with X-ray microanalysis (SEM-EDX) and micro X-ray fluorescence (µXRF), crystalline phases were identified by micro X-ray diffraction (µXRD), and the local structure of Zn and Cd were studied by Zn K-edge µEXAFS and Cd L_{III}-edge µXANES spectroscopy, respectively.

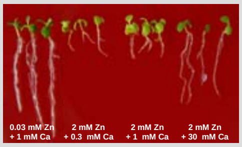

Figure 1: Comparison of tobacco seedlings exposed to various Zn and Ca concentrations. The growth inhibition induced by the exposure to 2 mM Zn is partially suppressed by a high Ca concentration (30 mM), which indicates a protective effect of ca against Zn toxicity.

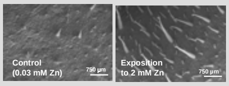

Figure 2: Comparison of leaf surfaces of tobacco exposed to 0.03 and 2 mM Zn by VP-SEM. The high Zn exposure induces an increase in the trichome density and in the number of grains excreted.

Figure 3: Grain excreted through tobacco trichomes.

MATERIALS AND METHODS

Tobacco were grown for 5 weeks in hydroponic solutions containing various Ca, Zn and Cd concentrations. After harvesting, grains present on the leaves were isolated by water extraction.

For the **SEM-EDX** analyses, isolated grains were attached on a carbon stub with carbon tape, and coated with carbon, and analyzed with a Jeol JSM 840A microscope fitted with a Kevex Si (Li) X-ray detector at an accelerating voltage of 15 kV.

The **µXRF, µXRD and Zn K-edge µEXAFS** experiments were performed on beamline 10.3.2 of the Advanced Light Source (ALS), Berkeley, CA (Marcus et al., 2004). For the µXRF and µEXAFS measurements, the beam was focused down to 5 × 5 µm and the X-ray fluorescence was measured with a 7-element Ge detector. For the µXRD measurements, the diffraction patterns were recorded with a 1024 × 1024 pixels CCD camera at 17 keV incident X-ray energy with a 16 µm (H) x 7 µm (V) beam size.

The **Cd L_{III}-edge µXANES** experiments were conducted on beamline ID21 of the ESRF (Susini et al., 2002) under vacuum. The beam was focused down to 0.3 µm (V) x 0.5 µm (H) and the X-ray fluorescence signal was collected with a 1-element Ge detector.

RESULTS

SEM-EDX ANALYSIS OF THE GRAINS

Exposition to Zn + Ca

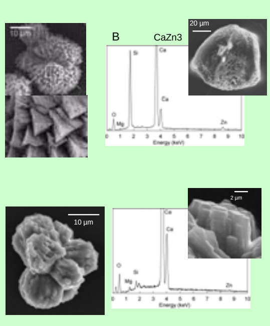

Figure 4: SEM images and EDX spectra of grains produced by tobacco exposed to (A) 0.03 mM Zn + 3 mM Ca, and (B, C) 0.25 mM Zn + 3 mM Ca.

Exposition to Cd + Ca

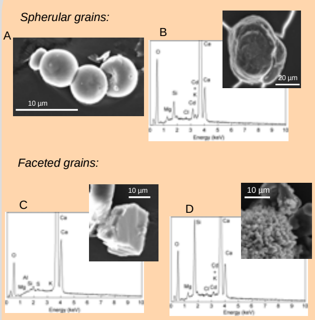

Figure 5: SEM images and EDX spectra of spherular (A, B) and faceted (C, D) grains produced by tobacco exposed to 0.25 mM Cd + 3 mM Ca.

Grains excreted under Zn + Ca exposition contain Ca, Zn, Mg, (Si) and sometimes Mn. Various morphologies are observed including faceted, spherular, and aggregates of particles.

For a Cd + Ca exposition, grains contain Ca, Mg, ± Cd, (Si). Two morphologies of grains are observed: spherular grains and faceted grains. Spherular grains are generally more enriched with Cd.

MICRO X-RAY DIFFRACTION

Exposition to Zn + Ca

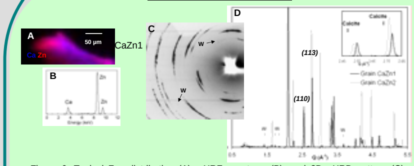

Figure 6: Typical Zn distribution (A), µXRF spectrum (B), and 2D µXRD pattern (C) of a grain (CaZn1). The analysis of the µXRD pattern (D) shows that grain CaZn1 and CaZn2 contain calcite with different degrees of substitution (inset in D), and CaZn1 contains whewellite as well.

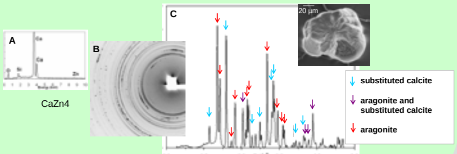

Figure 7: EDX spectrum (A), 2D µXRD pattern (B), and one-dimensional XRD pattern (C) for grain CaZn4. Aragonite and substituted calcite were identified.

Exposition to Cd + Ca

Spherular grains:

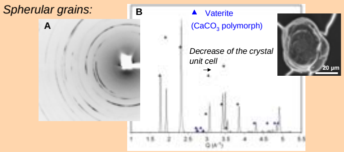

Figure 8: Typical 2D µXRD pattern (A) of a spherular grain. The analysis of the µXRD pattern (B) shows that the grain does not contain calcite but only substituted vaterite.

Faceted grains:

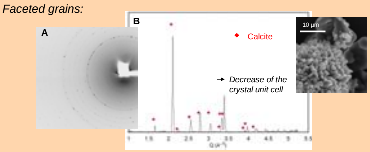

Figure 9: Typical 2D µXRD pattern (A) of a faceted grain. The analysis of the µXRD pattern (B) shows that the grain contains only substituted calcite.

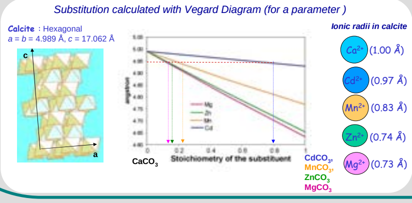

For Zn + Ca exposition, (Zn, Mg, Mn)- substituted calcite was the predominant mineral. Aragonite was rarely identified. For Cd + Ca treatment, (Cd, Mg)-substituted calcite was identified in faceted grains, and (Cd, Mg)-substituted vaterite was suggested in spherular grains.

Zn K-EDGE µEXAFS SPECTROSCOPY

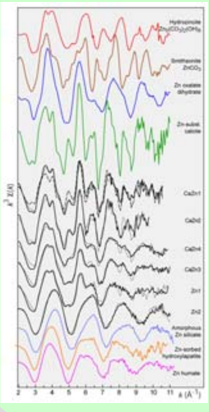

	Proportion of Zn species (%) determined by linear combination fitting the µEXAFS spectra						Elements detected by SEM-EDX and/or µXRF	Minerals identified by µXRD
	Zn-substituted calcite	Zn-organic acids	Zn-sorbed silica	Zn-sorbed phosphate	Sum	NSS (%) [a]		
CaZn1	53 40 44	- 50 -	- - -	- - 49	53 90 93	23.6 8.5 9.5[b]	Zn, Ca (light elements n.a.)	Subst. calcite ($Ca_{[illegible]}(Mg, Zn)_{[illegible]}CO_3$), whewellite (W, CaC_2O_4, H_2O)
CaZn2	50 53	39 -	- -	- 38	89 91	11.3 11.7[b]	Zn, Ca (light elements n.a.)	Subst. calcite ($Ca_{[illegible]}(Mg, Zn)_{[illegible]}CO_3$)
CaZn4	23	57	-	-	80	7.9	Zn, Ca, Si, O	Subst. calcite ($Ca_{[illegible]}Zn_{[illegible]}CO_3$)
CaZn3	22	78	-	-	100	7.2	Zn, Ca, Si, O	Subst. calcite ($Ca_{[illegible]}Zn_{[illegible]}CO_3$), aragonite ($CaCO_3$)
Zn1	15	73	-	-	88	4.8	Zn, Ca, K, Cl, Si, Mg, O	Subst. calcite ($Ca_{[illegible]}(Mg, Zn)_{[illegible]}CO_3$)
Zn2	-	37	79	-	115	2.7	Zn, Ca, K, Cl, Si, Mg, O	-

[a] Residual between fit and experimental data: $NSS = \Sigma [k^3\chi(k) - k^3\chi(k)_{fit}]^2 / \Sigma [k^3\chi(k)]^2 \cdot 100$. [b] Simulation not shown in the figure.

Figure 10: Zn bulk EXAFS spectra for selected Zn reference compounds, and Zn µEXAFS spectra for grains produced by tobacco exposed to 0.25 mM Zn + 3 mM Ca (**CaZn1, CaZn2, CaZn3 and CaZn4**) and to 0.25 mM Zn (**Zn1 and Zn2**) Solid line: experimental data, dashed line: one-component fit (for CaZn1 only), dotted line : two-component fit.

The presence of Zn-substituted calcite found by µXRD was confirmed by Zn µEXAFS spectroscopy, and three other Zn species were identified : Zn bound to organic compounds, and Zn-containing silica and phosphate.

Grains always contain a mixture of Zn species, and the proportion of Zn-substituted calcite relative to the other species increases with Ca exposure.

Cd L_{III}-EDGE µXANES SPECTROSCOPY

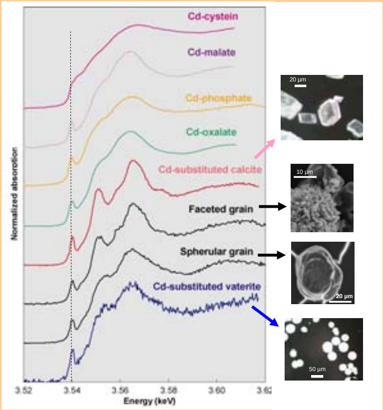

Figure 11: Cd L_{III}-edge XANES spectra for selected Cd reference compounds, and Cd µEXAFS spectra for spherular and faceted grains produced by tobacco exposed to 0.25 mM Cd + 3 mM Ca.

The presence of Cd-substituted calcite found by µXRD in faceted grains was confirmed by Cd µXANES spectroscopy. The occurrence of Cd-substituted vaterite in spherular grains was also corroborated by Cd µXANES spectroscopy. A mixture of Cd-substituted calcite and Cd-substituted vaterite was often identified.

CONCLUSIONS

The production of Cd- and Zn-containing biogenic calcium carbonates and other metal-containing compounds through the trichomes is a novel mechanism of metal detoxification. This finding has health and environmental significances since smoking is one of the main routes of exposure to metals, and tobacco is a candidate species for phytoremediation.

This study illustrates the potential of microfocused X-ray synchrotron radiation techniques to study biomineralization and metal homeostasis processes in plants, and the interest of combining complementary techniques such as µXRD, µXRF and µXAFS spectroscopy.

REFERENCES

Choi YE, Harada E, Kim G, Yoon E, Sano H (2004) Distribution of elements on tobacco trichomes and leaves under cadmium and sodium stresses. J. Plant Biol. 47: 75-82

Choi YE, Harada E, Wada M, Tsuboi H, Morita Y, Kusano T, Sano H (2001) Detoxification of cadmium in tobacco plants: formation and active excretion of crystals containing cadmium and calcium through trichomes. Planta 213: 45-50

Marcus MA, MacDowell AA, Celestre R, Manceau A, Miller T, Padmore HA, Sublett RE (2004) Beamline 10.3.2 at ALS: a hard X-ray microprobe for environmental and materials sciences. J. Synchrotron Rad. 11: 239-247

Susini J, Salome M, Fayard B, Ortega R, Kaulich B (2002) The scanning X-ray microprobe at the ESRF "x-ray microscopy" beamline. Surface Review and Letters 9: 203-211.

ACKNOWLEDGMENTS

We acknowledge the ALS and the ESRF for the provision of beamtime. E. Harada is a recipient of a BioGreen 21 Program and fellowships from the Human Frontier for Science Program (HFSP) and from the Alexander von Humboldt Foundation.

E-mail : mpisaure@ujf-grenoble.fr , gsarret@ujf-grenoble.fr, Phone: 00 33 4 76 82 80 21